Effect of Nozzle Geometry on Near-Field Modal Content of a Screeching Jet

Kyle A. Miller*, David Morata† and Dimitri Papamoschou.‡
University of California, Irvine, Irvine, CA, 92697

The acoustic near-field of a supersonic underexpanded jet at $M_j = 1.34$ was studied experimentally. A near-field azimuthal microphone array was utilized to study the jet oscillation dynamics and infer the geometrical pattern of the upstream-traveling acoustic waves involved in the jet screech mechanism. Operation of the jet in isolation resulted in a lateral oscillation (mode B) with an acoustic field containing strong screech tones. Addition of a conical reflector of 60° cone half-angle changed the oscillation dynamics, with new mode E appearing prominently and coexisting with mode B. The cross-spectral densities at the distinct tone frequencies are utilized to discern the jet oscillation dynamics and screech frequency and wavelength prediction formulas are utilized to assess if mode E is an extension of previously observed screech modes.

I. Nomenclature

a	=	speed of sound
D	=	nozzle exit diameter
f	=	cyclic frequency
G	=	cross-spectral density
M_j	=	fully-expanded jet Mach number
p	=	pressure fluctuation
P	=	Fourier transform of pressure fluctuation
r	=	radial coordinate
U_c	=	convective velocity
U_j	=	fully-expanded jet velocity
x	=	axial coordinate
λ	=	wavelength
θ	=	phase angle
ϕ	=	azimuthal coordinate
ω	=	angular frequency

II. Introduction

The operation of high performance aircraft necessitates propulsive devices that during some portion of the flight envelope operate under imperfectly-expanded conditions. During this flight regime, the supersonic jet exhaust generates noise through turbulent mixing and through the interaction of turbulent structures with the shock cells. Shock-associated noise is comprised of a broadband component, denoted as broadband shock associated noise (BBSAN) and strong tones referred to as screech. Screech tones are dangerous to personnel working in close proximity to the aircraft and are cited to cause damage to structures near the nozzle exit [1, 2] of tactical aircraft such as the F-15 fighter jets used by the United States Air Force. Effective minimization of the detrimental effects caused by these intense tones on military personnel and aircraft structures first requires a thorough understanding of how these tones are generated.

Screech tones were first observed in the pioneering work of Powell [3], who correctly argued that screech was generated by means of a feedback mechanism loop. An initial disturbance at the nozzle lip is convected downstream as a Kelvin-Helmholtz instability wave where it interacts with the tips of the shock-cell structure in a mechanism known

*Graduate Student Researcher, Mechanical and Aerospace Engineering, kamille2@uci.edu, Student Member AIAA.
†Graduate Student Researcher, Mechanical and Aerospace Engineering, dmoratac@uci.edu, Member AIAA.
‡Professor, Mechanical and Aerospace Engineering, dpapamos@uci.edu, Fellow AIAA.

as shock leakage [4, 5]. Through this mechanism, upstream and downstream propagating acoustic waves are generated with the directivity being highly dependent on the dynamics of the mode oscillation and the tone frequency. The upstream-propagating component ultimately closes the feedback loop through further excitation of the thin shear layer at the nozzle exit [1]. Previous work has observed screech generation to occur several shock-cells downstream of the nozzle lip [6] and at multiple locations [7, 8].

Many of these past studies have used an "effective source" location from which the upstream-propagating waves appear to be generated from. As discussed by Raman [7], this is not in conflict with the phased monopole array idea of Powell if such array has an acoustic center. However, the fact that screech appears to emanate from multiple shock-cells must be appropriately determined. Mercier *et al.* [9] used near-field data and optical tools to locate the effective acoustic source of screech between the third and fourth shock cell tips for a wide range of fully-expanded jet Mach numbers.

Previous studies have investigated how geometrical manipulation of the jet nozzle through the addition of reflectors or shielding surfaces near the nozzle exit alter the screech emission dynamics. Raman *et al.* [10] studied the feedback loop in rectangular nozzle geometries by using circular reflectors positioned upstream of the nozzle exit. They demonstrated how the reflector changes the position of the pressure node and anti-node, thus enhancing or suppressing screech emission. The presence of upstream reflecting surfaces also causes screech cessation and reactivation [11] and screech mode switches [12]. Complex reflecting geometries such as spherical [13] or conical reflectors [14, 15] have been also shown to change the screech emission dynamics. In particular, Morata and Papamoschou [15] noted how new screech modes might arise when installing conical reflector surfaces near the nozzle exit. Addition of these surfaces also minimized the tonal and BBSAN emissions for certain observation angles. However, the main new mode, which they categorized as mode E, has not been described azimuthally.

Prediction of the screech frequency has been a topic of intense research. For instance, Gao and Li [16] utilized the number of concurrent disturbances present at a given instance and the screech source location to predict the screech frequency for modes A1, A2, B, and C. Recent efforts using high-fidelity computational tools have aimed at obtaining near-field information of supersonic jet flows. Gojon and Bogey [17] studied a round underexpanded jet that contained two screech tones near mode C. Interest has also grown in the study of modal components of supersonic jets [18–21] for the prediction of the oscillation dynamics and screech frequency, and the study of the effects of heating [22] on supersonic jet flows. The prediction formula presented by Gao and Li [23] is utilized in this work to discern if oscillation mode E can be classified as an extension to previous screech tones that becomes re-excited by modifications to the geometry of the nozzle exit.

The aim of the present work is the investigation and the azimuthal characterization of oscillation mode E, which appears when placing conical reflector surfaces at the nozzle exit for some jet fully-expanded Mach numbers. A convergent nozzle is utilized, resulting in a jet operating in an underexpanded condition. Measurements are obtained utilizing a near-field azimuthal microphone array capable of capturing high resolution details of mode E.

III. Methodology

A. Harmonic Content

This work utilizes a near-field azimuthal microphone array positioned at multiple axial stations to study the oscillation dynamics of screeching jets issuing from nozzles having different exit geometries. Jet screech is manifested by highly localized frequency peaks in the Sound Pressure Level (SPL) spectrum. Besides the tone at the fundamental frequency of the resonant mode, one usually finds a richness of tones corresponding to integer multiples of the fundamental, each of them having clearly distinct directivity patterns. In some cases, an imperfectly-expanded round jet might show several tones corresponding to different modes. This multiplicity of modes has been seen in past experimental results [10, 24, 25]. The modes, and their corresponding tones, might be intermittent, and switching from one to another, being mutually exclusive for the duration of the experiment. However, it has been seen that multiple modes can be mutually co-existing in some instances [10]. To determine the characteristics of the jet for a specific tone, the tone is first located in frequency by searching for the maximum amplitude of SPL within a short frequency window surrounding the tone. The frequency corresponding to the maximum amplitude is designated as the tone frequency. The same frequency is used in constructing the tonal cross-spectral density (CSD).

B. Azimuthal Phase Decomposition

This study focuses on simultaneous azimuthal measurements of the near field pressure. Using the polar coordinate system (x, r, ϕ) depicted in Fig. 3, these pressure measurements are denoted $p(x, r, \phi_i, t)$, where for a given set of experiments x and r are fixed and the azimuthal angle takes discrete values ϕ_i. Omitting the arguments x and r for brevity, the Fourier transform of each pressure signal is denoted $P(\phi_i, \omega)$. The cross-spectral density (CSD) of sensors i and j is computed from

$$G_{ij}(\omega) = < P(\phi_i, \omega)\, P^*(\phi_j, \omega) > \tag{1}$$

where $< >$ denotes the spectral averaging and $(\,)^*$ is the complex conjugate.

The phase difference between two sensors is determined from

$$\Delta\theta_{ij} = \tan^{-1}\left(\frac{Im\{G_{ij}\}}{Re\{G_{ij}\}}\right) \tag{2}$$

where $Re\{\,\}$ and $Im\{\,\}$ are the real and imaginary components, respectively.

C. Screech Tone Classification

The label $\mathrm{X}^{(k)}$ is used here to designate a screech tone, where X is the mode and k is the harmonic. The mode notation of Ref. [26] is followed. Modes A1 and A2 denote torroidal oscillation. Modes B and C describe lateral and helical oscillations, respectively. Classification of screech tone $\mathrm{E}^{(1)}$ is attempted utilizing prediction formulas developed by Gao and Li [23] to estimate the screech frequency and wavelengths. Utilizing the number of concurrent disturbances and the screech source location, Gao and Li estimate the screech frequency for tones A1, A2, B, and C in circular jets as

$$f_s = \frac{m}{n\,L}\,\frac{U_c}{1 + U_c/a} \tag{3}$$

where a is the ambient speed of sound, U_c is the convective velocity number of the instability waves, L is the average shock-cell spacing, n is the number of shock-cell spacings defining the source region, and m is an integer representing the number of screech cycles. The ratio of the convective velocity to the jet fully expanded velocity, U_c/U_j, falls in the range $0.64 \leq U_c/U_j \leq 0.80$ and some guidance is offered on its selection based on mode. For modes A1, A2, B, and C the value $n = 5$ was proposed, with the shock-cell spacing given as

$$\frac{L}{D} = 1.26\,\sqrt{M_j^2 - 1} \tag{4}$$

where M_j is the fully-expanded jet Mach number. The screech wavelength is obtained simply from

$$\lambda_s = \frac{a}{f_s} \tag{5}$$

IV. Experimental Setup

A. Jet Flow

This study examined underexpanded round jets issuing from a convergent nozzle with exit diameter $D = 14.2$ mm. The baseline (isolated) nozzle had a smooth outer surface that terminated with a lip thickness of 0.4 mm. A conical reflector was added to the baseline nozzle. The reflector had a base diameter of 60.0 mm ($4.22D$) and cone half-angle of 60°. Coordinates and pictures of the nozzles are shown in Figs. 1 and 2, respectively. The reflector surface was 3D printed using a Formlabs Form 2 printer and polished so that the surface roughness was much smaller than the screech acoustic wavelength. Structures upstream of the nozzle were covered with anechoic foam to minimize any reflections towards the nozzle. The nozzle was supplied by air at room temperature and total pressure $p_0 = 297$ kPa resulting in a fully-expanded Mach number $M_j = 1.34$ and fully-expanded velocity U_j=397 m/s. During each experimental run, the total pressure was held within 1% of its target value.

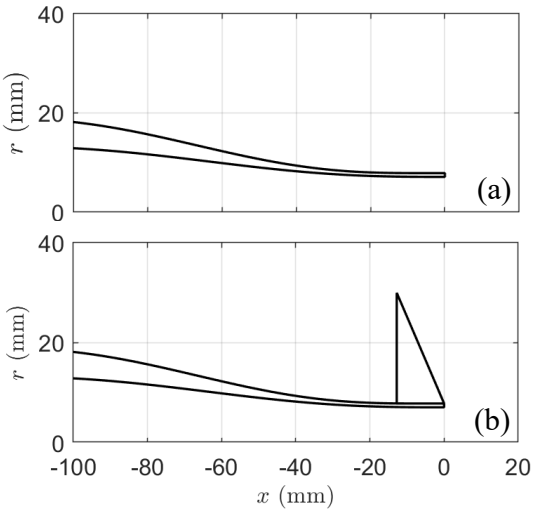

Fig. 1 Radial coordinates of the nozzles: (a) Isolated; and (b) with 60° conical reflector.

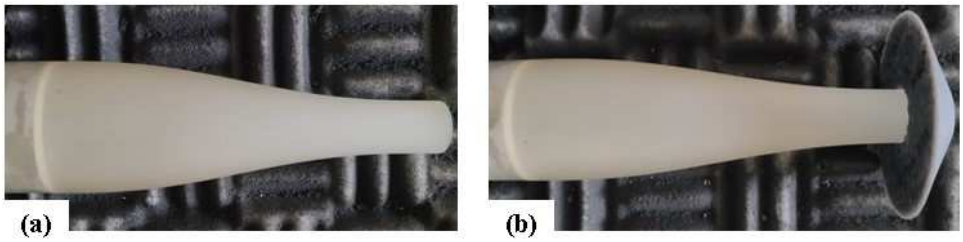

Fig. 2 Pictures of the nozzles: (a) Isolated; and (b) with 60° conical reflector.

B. Microphone Array

The experiments were conducted in the UCI Aeroacoustics Facility depicted in Fig. 3. The microphone array comprised of fifteen 1/8-inch condenser microphones (Brüel and Kjaer, Model 4138) with frequency response up to 120 kHz. The microphones are connected, in groups of four, to six conditioning amplifiers (Brüel and Kjaer, Model 2690-A-0S4). The outputs of the amplifiers are sampled simultaneously, at 250 kHz per channel, by three 8-channel multi-function data acquisition boards (National Instruments PCI-6143) installed in a computer with an Intel i7-7700K quad-core processor. National Instruments Labview software provided the interface for signal acquisition and filtering, as well as control of the experiment. The microphone signals are conditioned with a high-pass filter set at 350 Hz to remove any spurious noise. Temperature and humidity inside the chamber are recorded to enable the calculation of the effects of atmospheric absorption.

The microphones were mounted on a ring holder to investigate the azimuthal structure of the near pressure filed, as depicted in Figs. 3 and 4. For all the experiments the microphone sensors were located at a non-dimensional radius $r/D = 4.71$ from the jet centerline. A total azimuthal aperture of 201.6° was covered, where the azimuthal angle ϕ is measured positive clockwise from the horizontal plane as shown in Fig. 3. The azimuthal increment between sensors was uniformly set at 14.4°. The ring array was placed at nine uniformly spaced axial stations, $x/D = 0, 1, \ldots, 8$.

The microphones were sampled simultaneously at a rate of 250000 samples per second. The acquisition time was 2 s. Sound Pressure Level (SPL) spectra and cross-spectral densities were computed using a Fast Fourier Transform (FFT) size of 2048, giving a frequency resolution of 122 Hz. The SPL spectra were corrected for actuator response, microphone free-field correction and atmospheric absorption.

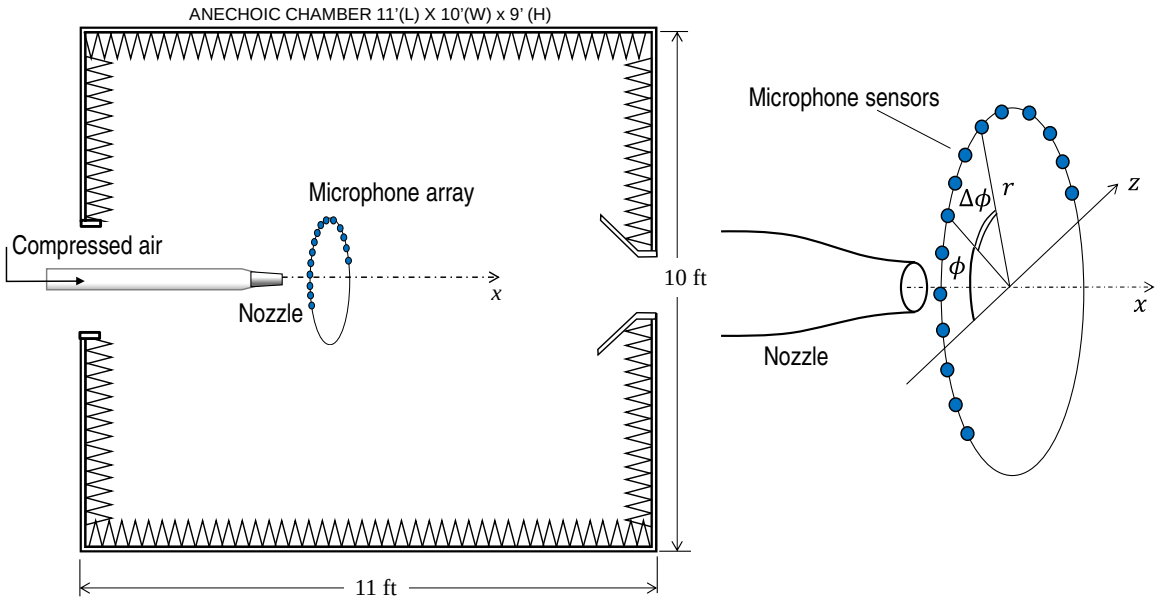

Fig. 3 Schematic of near-field microphone phased array deployment inside the UCI anechoic chamber. The array was translatable in x.

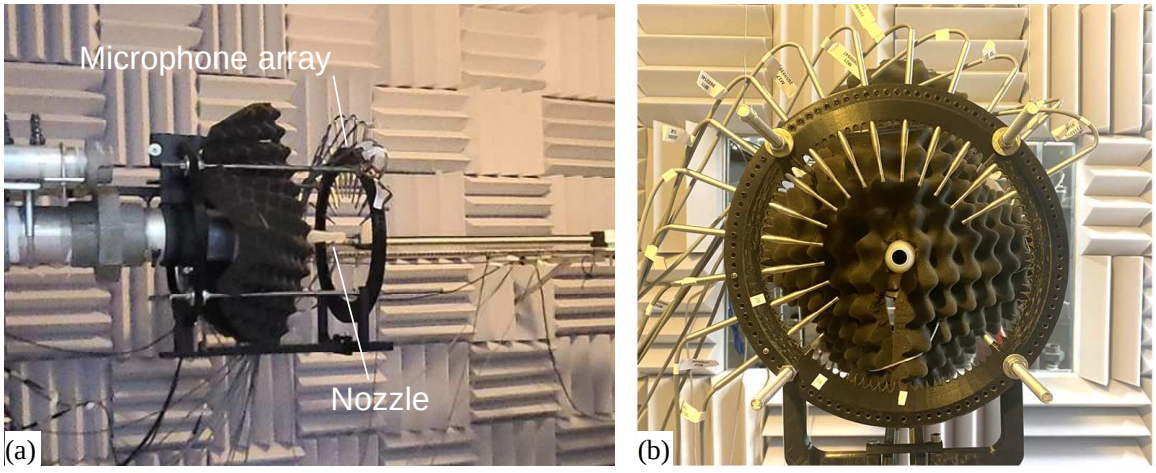

Fig. 4 Photographs of the jet rig and microphone array. (a) Perspective view; (b) view from downstream.

V. Results

A. Sound Pressure Level Spectra

The impact of the reflector on the near-field emission is exemplified by the SPL spectra at $x/D = 0$ and $\phi = 127.8°$. Figure 5 plots the SPL spectra at this location for the isolated jet and the jet with the 60° reflector. For the isolated jet, tones $B^{(1)}$ and $B^{(2)}$ are prominent, with tone $B^{(3)}$ making a weak appearance. The frequency of $B^{(1)}$ is 9032 Hz. Addition of the reflector results in a dramatic change where mode B is almost completely suppressed, with $B^{(1)}$ barely surviving. Instead, mode E arises with tones $E^{(1)}$ and $E^{(2)}$ appearing prominently. The frequency of $E^{(1)}$ is 11597 Hz. These results are in line with far-field measurements of screech tones for the same nozzle conditions [14].

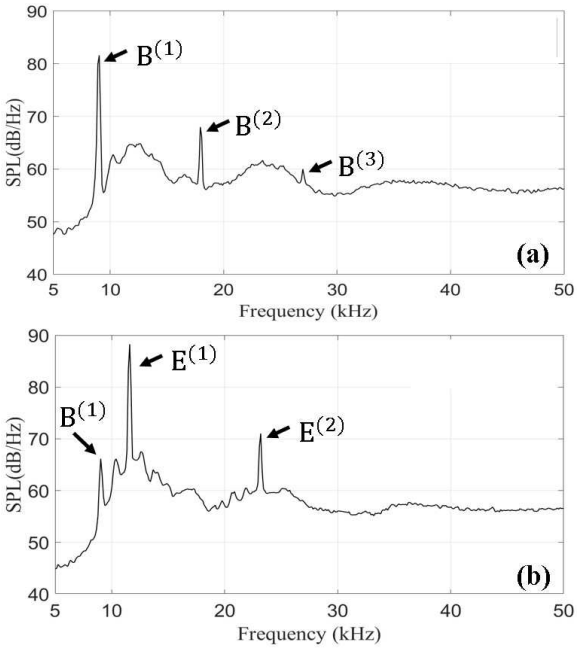

Fig. 5 SPL spectra at $x/D = 0$, $r/D = 4.71$, $\phi = 127.8°$. (a) Isolated jet; (b) jet with 60° reflector.

Focusing now on the tonal content, the axial and azimuthal evolution of the SPL for various tones is presented in Fig. 6. Referring to Fig. 6a, tone $B^{(1)}$ shows a significant decline with x/D and there is appreciable variation with azimuthal angle. The latter may be due to the flapping oscillation, associated with mode B, occurring on a fairly constant plane during the short duration of the experiment. Addition of the reflector suppresses greatly tone $B^{(1)}$ near $x/D = 0$, as seen in Fig. 6b, with some rise occurring at downstream stations. The azimuthal variation is not as pronounced as in the isolated case. Regarding mode E, tone $E^{(1)}$ starts very strong and shows a moderate decline with x/D but with significant bumps whose origin cannot be ascertained at this point (Fig. 6c). Tone $E^{(2)}$ shows a smoother progression with x, declining initially and then rising to high level (Fig. 6d). Generally, the azimuthal variation of SPL with the reflector is less than for the isolated jet. This is consistent with either an axisymmetric mode or a flapping mode whose plane shifts rapidly.

B. Mode Characteristics

The oscillation patterns of the jets were examined utilizing the azimuthal array at multiple axial locations. Screech tones are known for containing high-intensity acoustic components that propagate in the upstream direction. This information can be utilized to discern the oscillation characteristics of the jet flow. First, the CSD between a center microphone ($\phi = 66.6°$) and the remaining microphones is calculated using the procedure in section III.B. The phase difference is calculated at the frequency of the desired tone from Eq. 2. By displaying the phase difference as a function of the azimuthal spacing, the jet oscillation dynamics can be unveiled [27]. In the case of symmetric oscillations, the values for $\Delta\theta$ are expected to cluster near 0 for all microphone separations $\Delta\phi$, indicating the presence of plane waves

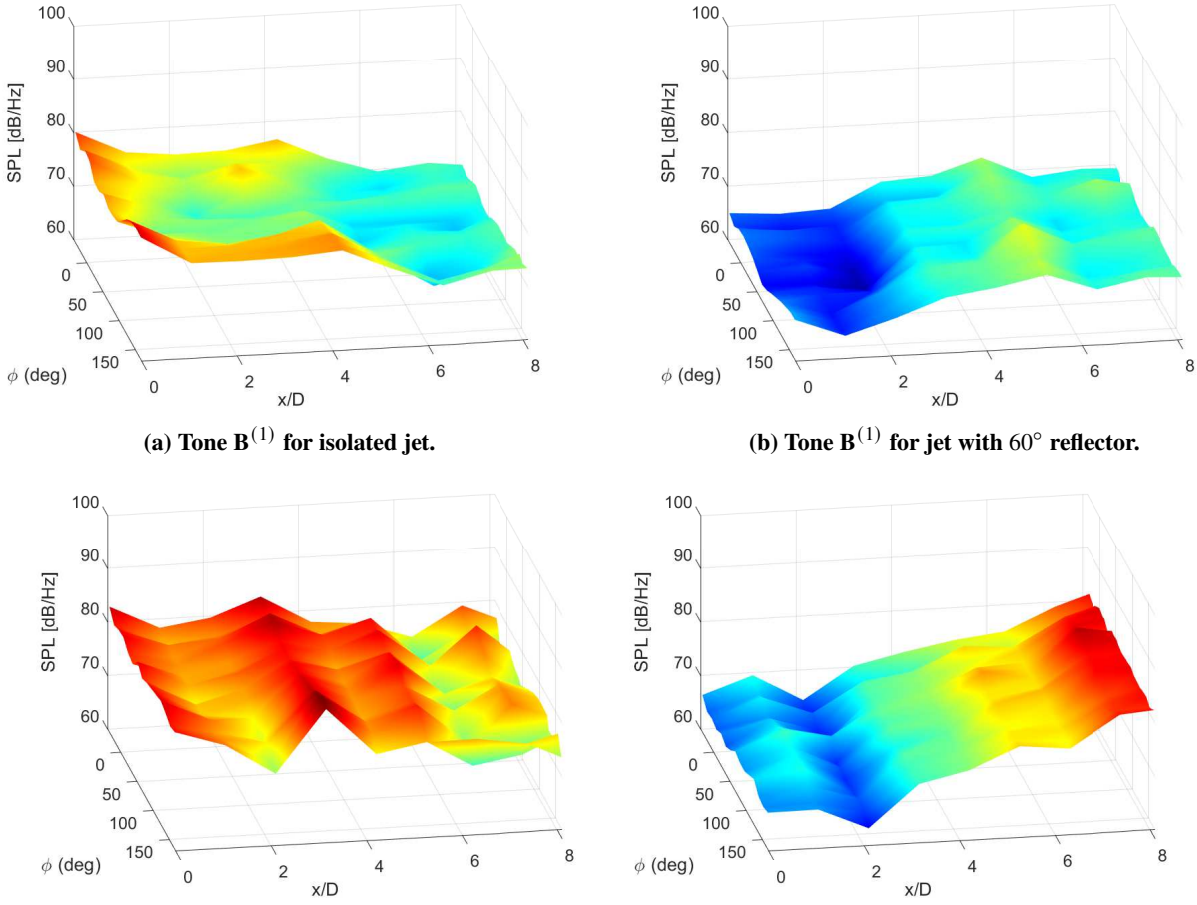

(a) Tone $B^{(1)}$ for isolated jet.

(b) Tone $B^{(1)}$ for jet with 60° reflector.

(c) Tone $E^{(1)}$ for jet with 60° reflector.

(d) Tone $E^{(2)}$ for jet with 60° reflector.

Fig. 6 Surface plots of tonal SPL versus x/D and ϕ.

reaching the nozzle exit. Lateral jet oscillations are expected to result in phase differences either clustering near 0 or near $\pm 180^\circ$ [27] indicating the presence of a flapping jet.

Plots of phase difference versus azimuthal spacing at four axial stations are presented in Fig. 7 for tone $B^{(1)}$ of the isolated jet and tones $E^{(1)}$ and $E^{(2)}$ for the 60° reflector. At $x/D = 0$, the phase difference for tone $B^{(1)}$ is near zero for $0 \leq \Delta\phi \leq 100^\circ$ and increases with negative $\Delta\phi$, reaching $\Delta\theta = 180^\circ$ at $\Delta\phi = -90^\circ$. This suggests lateral oscillations which would be consistent with the nature of mode B. For the downstream stations, tone $B^{(1)}$ sustains a significant phase difference across the measured $\Delta\phi$, with a trend reversal at $x/D = 3$. When the reflector is installed, tone $E^{(1)}$ displays modest variations in $\Delta\theta$, suggesting mostly plane waves traveling upstream. Tone $E^{(2)}$ shows a phase variation similar to that of $E^{(1)}$ near $x/D = 0$, but the phase variation amplifies with downstream distance, becoming similar to that of $B^{(1)}$ for the isolated jet. This result suggests that the addition of the 60° reflector introduces disturbances to the upstream propagating acoustic waves that causes high-frequency lateral oscillations downstream to transition into mostly plane waves before reaching the nozzle exit. The existence of plane acoustic waves near the nozzle exit additionally suggest a possibility that mode E is an extension of previously encountered toroidal modes, the tones of which get reactivated with the addition of the reflector.

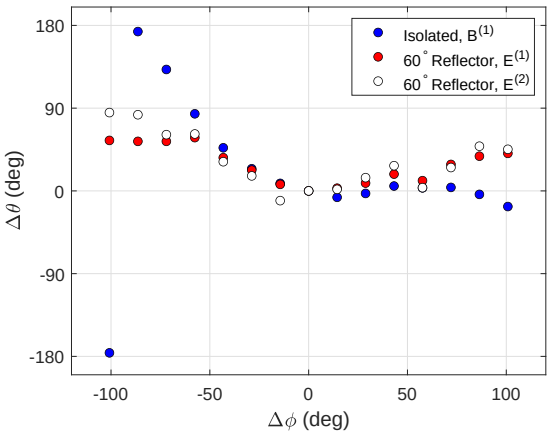

(a) Azimuthal phase difference for $x/D = 0$

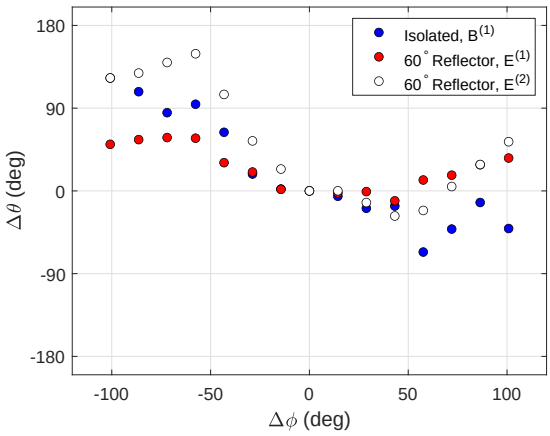

(b) Azimuthal phase difference for $x/D = 3$

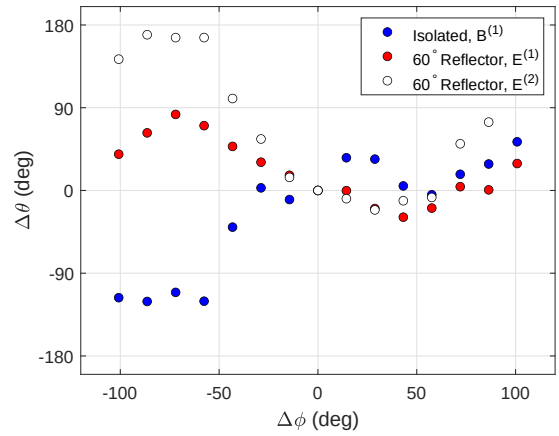

(c) Azimuthal phase difference for $x/D = 5$

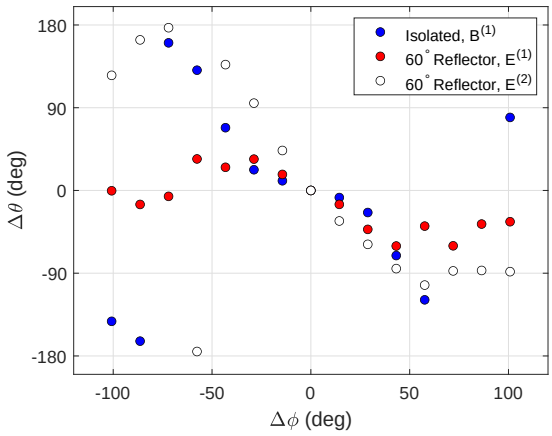

(d) Azimuthal phase difference for $x/D = 8$

Fig. 7 Phase variation between sensor azimuthal angles at four axial locations.

C. Modal Content

The toroidal nature for tone $E^{(2)}$ inferred by the results in Section V.B suggests the possibility that mode E could be an extension of mode A2 (toroidal mode)[23] that becomes re-excited by the geometrical modification of the 60° conical reflector. Using Eq. 3 with parameters specific to the axisymmetric mode A2 ($m = 6$, $n = 5$, $U_c/U_j = 0.67$, $M_j = 1.34$) [23], the frequency of tone $E^{(1)}$ is predicted to be 11249 Hz, a 3.0% difference from the measured frequency of 11597 Hz. Using the same parameters, Fig. 8 compares the predicted screech wavelength obtained from Eq. 3 with measured wavelengths of tone A2 obtained from [23] and the measured wavelength of tone $E^{(1)}$. The figure suggests that the wavelength of $E^{(1)}$ follows the trend of the wavelengths measured for tone A2. Despite this promising result, further work is needed to demonstrate rigorously that $E^{(1)}$ is an extension of A2.

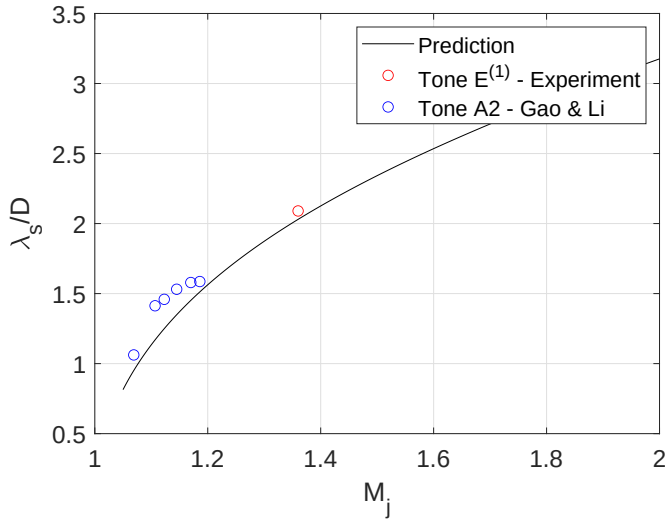

Fig. 8 Wavelength of tone $E^{(1)}$ compared to prediction formula and wavelengths of mode A2 by Gao and Li [23].

VI. Conclusions

The modal structure of a screeching underexpanded jet with $M_j = 1.34$, and its modification by altering the nozzle geometry, was investigated using a near-field azimuthal microphone array. The array comprised 15 microphones located at azimuthal increments of 14.4°. It was placed at nine axial locations covering the region $x/D = 0$ to 8. Alteration of the nozzle geometry came in the form of a 60° conical reflector. Measurements of the sound pressure level (SPL) spectrum and the cross-spectral density (CSD) were performed for all the stations. The phase difference between sensors was computed from the CSD. The isolated jet is dominated by mode B whose lateral oscillation characteristics are indicated by a large variation in phase angle over the angular aperture of the array. Installation of the reflector suppresses mode B and gives rise to mode E. The phase variations for mode E indicate strong lateral oscillations at downstream stations evolving into mostly axisymmetric disturbances near the nozzle exit. The presumed toroidal nature of mode E suggests that it may be an extension of previously known axisymmetric mode A2. The measured frequency of tone $E^{(1)}$ can be inferred from a screech frequency prediction formula using the parameters of mode A2. Further work is needed to confirm possible connections between modes A2 and E.

Acknowledgments

This work was partially supported by NASA Phase II Small Business Innovation Research (SBIR) contract 80NSSC20C0089 under technical monitor Dr. David Stephens of NASA GRC. ATA Engineering, Inc. was the prime.

References

[1] Raman, G., "Supersonic Jet Screech: Half-Century from Powell to the Present," *Journal of Sound and Vibration*, Vol. 225, No. 3, 1999, pp. 543–571. doi:10.1006/jsvi.1999.2181.

[2] Manning, T., and Lele, S., "A numerical investigation of sound generation in supersonic jet screech," *AIAA Paper 2000-2081*, 2000. doi:10.2514/6.2000-2081.

[3] Powell, A., "On the Mechanism of Choked Jet Noise," *Proc. Phys. Soc. London*, Vol. 26, 1953, pp. 1039–1056.

[4] Suzuki, T., and Lele, S. K., "Shock Leakage Through an Unsteady Vortex-laden Mixing Layer: Application to Jet Screech," *Journal of Fluid Mechanics*, Vol. 490, 2003, p. 139–167. doi:10.1017/S0022112003005214.

[5] Edgington-Mitchell, D., Weightman, J., Lock, S., Kirby, R., Nair, V., Soria, J., and Honnery, D., "The Generation of Screech Tones by Shock Leakage," *Journal of Fluid Mechanics*, Vol. 908, 2021, p. A46. doi:10.1017/jfm.2020.945.

[6] Tam, C. K. W., Parrish, S. A., and Viswanathan, K., "Harmonics of Jet Screech Tones," *AIAA Journal*, Vol. 52, No. 11, 2014, pp. 2471–2479. doi:10.2514/1.J052850.

[7] Raman, G., "Screech Tones from Rectangular Jets with Spanwise Oblique Shock-Cell Structures," *AIAA Paper 1996-0643*, 1996. doi:10.2514/6.1996-643.

[8] Edgington-Mitchell, D., Weightman, J., Lock, S., Kirby, R., Nair, V., Soria, J., and Honnery, D., "The Generation of Screech Tones by Shock Leakage," *Journal of Fluid Mechanics*, Vol. 908, 2020. doi:10.1017/jfm.2020.945.

[9] Mercier, B., Castelain, T., and Bailly, C., "Experimental Characterisation of the Screech Feedback Loop in Underexpanded Round Jets," *Journal of Fluid Mechanics*, Vol. 824, 2017, p. 202–229. doi:10.1017/jfm.2017.336.

[10] Raman, G., "Screech Rones from Rectangular Jets with Spanwise Oblique Shock-Cell Structures," *Journal of Fluid Mechanics*, Vol. 330, 1997, p. 141–168. doi:10.1017/S0022112096003801.

[11] Raman, G., "Cessation of Screech in Underexpanded Jets," *Journal of Fluid Mechanics*, Vol. 336, 1997, pp. 69–90. doi:10.1017/S002211209600451X.

[12] Edgington-Mitchell, D., "Aeroacoustic Resonance and Self-Excitation in Screeching and Impinging Supersonic Jets – A Review," *International Journal of Aeroacoustics*, Vol. 18, No. 2-3, 2019, pp. 118–188. doi:10.1177/1475472X19834521.

[13] Islam, M. T. K., and Seto, K., "Control of Supersonic Jet Noise with a Spherical Reflector," *The Journal of the Acoustical Society of America*, Vol. 116, No. 4, 2004, pp. 2539–2540. doi:10.1121/1.4785132.

[14] Morata, D., and Papamoschou, D., "Effect of Nozzle Geometry on the Space-Time Emission of Screech Tones," *AIAA Paper 2021-2306*, 2021. doi:10.2514/6.2021-2306.

[15] Morata, D., and Papamoschou, D., "Extension of Traditional Beamforming Methods to the Continuous-Scan Paradigm," *AIAA Paper 2022-1154*, 2022.

[16] Gao, J. H., and Li, X. D., "A Multi-Mode Screech Frequency Prediction Formula for Circular Supersonic Jets," *The Journal of the Acoustical Society of America*, Vol. 127, No. 3, 2010, pp. 1251–1257. doi:10.1121/1.3291001.

[17] Gojon, R., and Bogey, C., "Numerical study of the flow and the near acoustic fields of an underexpanded round free jet generating two screech tones," *International Journal of Aeroacoustics*, Vol. 16, No. 7-8, 2017, pp. 603–625. doi:10.1177/1475472X17727606.

[18] Chakrabarti, S., Gaitonde, D., and Unnikrishnan, S., "Representing Rectangular Jet Dynamics Through Azimuthal Fourier Modes," *Phys. Rev. Fluids*, Vol. 6, 2021, p. 074605. doi:10.1103/PhysRevFluids.6.074605.

[19] Chakrabarti, S., Gaitonde, D. V., and Unnikrishnan, S., "Wavepacket Dynamics in Rectangular Jets," *AIAA Paper 2022-2403*, 2022. doi:10.2514/6.2022-2403.

[20] Stahl, S. L., Prasad, C., and Gaitonde, D. V., "Feedback Mechanisms in a Supersonic Impinging Jet using Conditional Proper Orthogonal Decomposition," *AIAA Paper 2022-1153*, 2022. doi:10.2514/6.2022-1153.

[21] Prasad, A. L. N., Saleh, Y., Sellappan, P., Nair, U. S., and Alvi, F. S., "Near-field and far-field effects of heating in an over-expanded Mach 2 diamond jet." *AIAA Paper 2022-1152*, 2022. doi:10.2514/6.2022-1152.

[22] Prasad, A. L. N., Saleh, Y., Sellappan, P., Nair, U. S., and Alvi, F. S., "Near-Field and Far-Field Effects of Heating in an Over-Expanded Mach 2 Diamond Jet," *AIAA Paper 2022-1152*, 2022. doi:10.2514/6.2022-1152.

[23] Gao, J., and Li, X., "A Multi-Mode Screech Frequency Prediction Formula for Circular Supersonic Jets," *AIAA Paper 2009-3374*, 2009. doi:10.2514/6.2009-3374.

[24] Walker, S. H., and Thomas, F. O., "Experiments Characterizing Nonlinear Shear Layer Dynamics in a Supersonic Rectangular Jet Undergoing Screech," *Physics of Fluids*, Vol. 9, No. 9, 1997, pp. 2562–2579. doi:10.1063/1.869373.

[25] Chen, Z., Wu, J.-H., Ren, A.-D., and Chen, X., "Mode-Switching and Nonlinear Effects in Supersonic Jet Noise," *AIP Advances*, Vol. 8, No. 1, 2018, p. 015126. doi:10.1063/1.5010829.

[26] Seiner, J. M., Manning, J. C., and Ponton, M. K., "Dynamic Pressure Loads Associated with Twin Supersonic Plume Resonance," *AIAA Journal*, Vol. 26, No. 8, 1988, pp. 954–960. doi:10.2514/3.9996.

[27] Umeda, Y., and Ishii, R., "On the sound sources of screech tones radiated from choked circular jets," *The Journal of the Acoustical Society of America*, Vol. 110, No. 4, 2001, pp. 1845–1858. doi:10.1121/1.1402620.